AD-A134 927 APPLICATION OF RAPIDLY SOLIDIFIED SUPERALLOYS(U) PRATT 1/
AND WHITNEY AIRCRAFT GROUP WEST PALM BEACH FL
GOVERNMENT PRODUCTS DIV A R COX ET AL. FEB 78
UNCLASSIFIED PWA-FR-9744 F33615-76-C-5136 F/G 11/6 NL

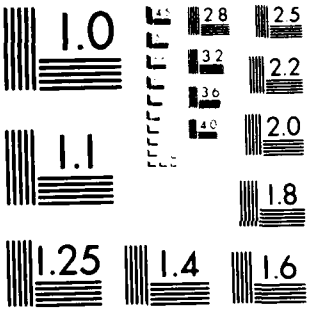

REPORT DOCUMENTATION PAGE

READ INSTRUCTIONS BEFORE COMPLETING FORM

Field	Entry
1. REPORT NUMBER	FR-9744
2. GOVT ACCESSION NO.	AD-A034327
3. RECIPIENT'S CATALOG NUMBER	
4. TITLE (and Subtitle)	APPLICATION OF RAPIDLY SOLIDIFIED SUPERALLOYS
5. TYPE OF REPORT & PERIOD COVERED	Quarterly Report 1 November 1977 – 31 January 1978
6. PERFORMING ORG. REPORT NUMBER	FR-9744
7. AUTHOR(s)	A. R. Cox E. H. Aigeltinger T. Tillman (contributing) W. K. Forrester (contributing)
8. CONTRACT OR GRANT NUMBER(s)	F33615-76-C-5136
9. PERFORMING ORGANIZATION NAME AND ADDRESS	United Technologies Corporation Pratt & Whitney Aircraft Group Government Products Division Box 2691, West Palm Beach, Florida 33402
10. PROGRAM ELEMENT, PROJECT, TASK AREA & WORK UNIT NUMBERS	
11. CONTROLLING OFFICE NAME AND ADDRESS	Defense Advanced Research Projects Agency 1400 Wilson Boulevard Arlington, Virginia 22209 (Dr. E. C. vanReuth)
12. REPORT DATE	February 1978
13. NUMBER OF PAGES	27
14. MONITORING AGENCY NAME & ADDRESS (if different from Controlling Office)	Air Force Materials Laboratories Wright-Patterson Air Force Base, Ohio 45433 (Mr. A. Adair)
15. SECURITY CLASS. (of this report)	Unclassified
15a. DECLASSIFICATION/DOWNGRADING SCHEDULE	
16. DISTRIBUTION STATEMENT (of this Report)	Approved for Public Release, Distribution Unlimited
17. DISTRIBUTION STATEMENT (of the abstract entered in Block 20, if different from Report)	
18. SUPPLEMENTARY NOTES	
19. KEY WORDS (Continue on reverse side if necessary and identify by block number)	Superalloys, Powder Metallurgy, Rapid Solidification, Turbine Airfoils, Centrifugal Atomization, Convective Cooling

Accession For	
NTIS GRA&I	☑
DTIC TAB	☐
Unannounced	☐
Justification	
By	
Distribution/	
Availability Codes	
Dist	Avail and/or Special
A-1	

DTIC COPY INSPECTED

20. ABSTRACT (Continue on reverse side if necessary and identify by block number)

This program is being conducted for the purpose of applying the principle of rapid solidification to superalloy powders and subsequent development of a stronger alloy composition for jet engine turbine airfoils. Centrifugal atomization and forced convective cooling are being used to produce the fast-cooled material.

During this report period, alloy iterations of the conventional and Ni-Al-Mo series were conducted; further work was conducted on phase thermal stability, grain orientation features, and forgeability. Creep-rupture testing continued with major results showing that Ta additions to Ni-Al-Mo alloys promote a stable phase dispersion up to the temperatures of γ' dissolution and early indications suggest that significant creep resistance is derived by the evolved Ni-Al-Mo-Ta microstructures.

SUMMARY

This program is being conducted for the purpose of applying the principle of rapid solidification to superalloy powders and subsequent development of a stronger alloy composition for jet engine turbine airfoils. Centrifugal atomization and forced convective cooling are being used to produce the fast-cooled material.

During this report period, alloy iterations of the conventional and Ni-Al-Mo series were conducted; further work was conducted on phase thermal stability, grain orientation features, and forgeability. Creep-rupture testing continued with major results showing that Ta additions to Ni-Al-Mo alloys promote a stable phase dispersion up to the temperatures of γ' dissolution and early indications suggest that significant creep resistance is derived by the evolved Ni-Al-Mo-Ta microstructures.

TABLE OF CONTENTS

SECTION I

INTRODUCTION

The performance improvements of current military gas turbines, such as the Pratt & Whitney Aircraft F100 engine, over earlier engines were made possible through advancements in design technology and materials processing. Better alloys, by virtue of chemical composition, played only a minor role in achieving the present capability. Future engine projections, however, demand that better materials be developed to achieve still higher levels of performance.

The turbine module is especially dependent on improvements in such alloy properties as high-temperature capability, better stability, and better corrosion resistance. The alloys presently being used in the turbine module were developed more than 15 years ago. These alloys are still in use, not because of a lack of interest in development but, rather, due to the inability to improve the nature of alloying under conditions now imposed for subsequent processing and component fabrication. Precision casting alloy compositions are limited because of such constraints as crucible and mold interactions and massive phase occurrence. Forging alloys are limited because of constraints of segregation during ingot processing.

Superalloy powder metallurgy studies conducted at the P&WA/Florida facility have shown that the use of powder, particularly powder solidified at very high rates of cooling, can eliminate the constraints noted and enable more effective alloying for the improvement of basic material properties. Several examples which support this statement are:

1. Chemical segregation in fast-cooled superalloy powders can be controlled to a submicron level.

2. Massive phases can be eliminated.

3. Solubility of alloying elements can be extended without deleterious phase reaction.

4. None of these can be achieved in ingot or precision casting.

Further, the inherent homogeneity of the powder indicates that subsequent processing and heat treatment can be used effectively to promote maximum material utilization. Abnormal grain growth, for example, can be achieved in superalloy powder materials for optimization of mechanical properties above $\frac{1}{2}$ T_m. MAR M200 alloy powder, processed and reacted in this manner, is, in fact, stronger than and as ductile as the same composition cast in a directional mode.

P&WA/Florida has constructed a device that can produce metal powders solidified and cooled at rates in excess of 10^6°C/sec. The underlying principle is forced convective cooling, whereby liquid particles of controlled size are accelerated into a high thermal conductivity gaseous medium maintained at high ΔT between itself and the particles.

The purpose of this Advanced Research Projects Agency (ARPA) sponsored program is to refine the process mechanics used with the powder producing device for fast-quenching bulk lots of powder and, subsequently, applying the technology of rapid solidification to the development of an alloy composition that is stronger than the existing MAR M200 alloy and that can be implemented for the production of better turbine airfoils.

The program is a 40-month effort and is organized as a progression of events starting with a parametric study of the requirements necessary to achieve high yields of fast-quenched powder and terminating in the fabrication and testing of turbine airfoils. This is the eighth technical report and covers the 22nd through 24th months of the program. It deals with the evaluation of experimental alloys, produced as fast-cooled powders.

SECTION II

MATERIALS EVALUATION

ALLOY SCREENING

The previous reports cited groundwork evaluation and testing of numerous alloys which represented four basic alloy systems. These were: (1) conventional superalloy compositions, (2) alloys commonly referred to as superalloy eutectics, (3) ternary Ni-Al-Mo alloys and, (4) simple, high volume fraction γ' alloys. These classes, and the specific alloys, were selected at the onset of the alloy study phase of the program to determine what type of response each would have with respect to rapid solidification and subsequent processing, phase reactions, etc.

For all classes, rapid solidification produced a starting material which was essentially a supersaturated solid solution. Subsequent consolidation by extrusion typically resulted in sound barstock. Heat treat studies showed further that all but the eutectic class of materials could be forced to undergo abnormal grain growth. Additionally, for the Ni-Al-Mo series, it was found that phase reactions, which were not expected for the specific alloy compositions, took place and contributed significantly to strengthening under conditions of creep at high temperature.

The overall results of testing of alloys previously reported led us to additional composition modification studies along three avenues. These included (1) modifications of major elements in a conventional type superalloy (we used RSR 121, whose base composition is alloy AF2-1DA), (2) secondary additions to the Ni-Al-Mo system, and (3) eutectics containing niobium. Twenty-two compositions were identified and processed during this period and were selected in a fashion representative of factorial experimentation. The alloys are listed in Table 1.

The alloy study for the conventional superalloy base was conducted principally to determine how the secondary phase (γ'), with Ta additions, could be modified. The design of the experiment is shown in Figure 1. Four factors were considered: (1) the concentration of Co, (2) the (Ti + Ta)/Al ratio, (3) the Ti/Ta ratio, and (4) the total concentration of Al, Ti, and Ta. The complete experiment, with all interactions accounted for, covers 81 individual alloys. This was considered unwieldy for our purposes and, accordingly, the specific compositions were randomized to a total of nine. These, also, are shown in the figure.

Tantalum was also considered as an alloying addition to the Ni-Al-Mo ternary and the experimental selection is shown in Figure 2. The base in this study was the alloy RSR 104 and individual concentrations of Ta, Al, and Mo were the principal considerations.

The niobium alloys were selected from published literature, with the exception of RSR 156 and 157, which were included to determine noibium substitution effects for Mo in the previously reported Ni-Al-Mo series. Alloy 151 was a high γ' composition which was run to complete the basic study reported earlier for the RSR 110 series of alloys.

As with the previous alloy runs, the operations to produce rapidly solidified powders proceeded with no discernible difficulties. And, as before, the characteristics of the powders were those of supersaturated solid solutions.

TABLE 1. SUPERALLOY COMPOSITIONS

Element (wt %*)

ID	*Ni*	*Co*	*Cr*	*Al*	*Ti*	*C*	*B*	*Mo*	*Zr*	*Ta*	*W*	*Nb*	*Category*
132	Bal	5.1	10.9	5.0	3.9	0.29	0.019	3.3	0.12	1.8	6.4	-	1
133	Bal	-	10.5	4.2	2.5	0.28	0.018	3.2	0.12	4.7	6.2	-	1
134	Bal	5.1	10.9	5.0	3.9	0.29	0.019	3.3	0.13	1.9	6.4	-	1
135	Bal	4.7	10.0	3.9	5.5	0.29	0.017	3.1	0.12	5.2	5.9	-	1
136	Bal	-	10.7	4.2	6.6	0.29	0.018	3.3	0.12	3.1	6.3		1
137	Bal	4.8	10.1	2.4	4.3	0.27	0.017	3.1	0.12	8.2	6.0	-	1
138	Bal	5.1	10.9	3.0	6.4	0.29	0.019	3.3	0.13	6.1	6.4	-	1
140	Bal	-	10.6	2.9	6.9	0.28	0.018	3.2	0.12	3.2	6.2	-	1
150	Bal	-	6.0	2.5	-	0.002	0.005	-	0.04	-	-	20.0	2
152	Bal	2.0	10.0	4.0	-	0.25	0.005	-	0.04	-	6.0	5.0	2
153	Bal	-	6.2	4.1	-	0.01	0.005	-	0.04	-	-	15.0	2
155	Bal	-	6.4	6.0	-	0.01	0.005	-	0.04	-	-	10.0	2
156	Bal	-	-	8.0	-	-	-	-	-	-	-	18.0	2
157	Bal	-	-	8.2	-	-	-	-	-	-	-	13.3	2
143	Bal	-	-	5.8	-	-	-	14.3	-	6.0	-	-	3
144	Bal	-	-	7.0	-	-	-	14.8	-	3.0	-	-	3
145	Bal	-	-	7.8	-	-	-	14.6	-	6.1	-	-	3
146	Bal	-	-	6.0	-	-	-	18.0	-	-	-	-	3
147	Bal	-	-	6.8	-	-	-	17.8	-	-	-	-	3
148	Bal	-	-	7.8	-	-	-	18.0	-	3.0	-	-	3
149	Bal	-	-	8.0	-	0.02	0.005	18.0	0.04	3.1	-	-	3
151	Bal	-	8.5	8.0	-	0.20	0.005	-	0.04	3.0	6.0	-	4

*Based on master heat charge weight

Category
1 Conventional Superalloy Type
2 DS Eutectic Type
3 Ni-Al-Mo Ternary Base
4 High γ Type

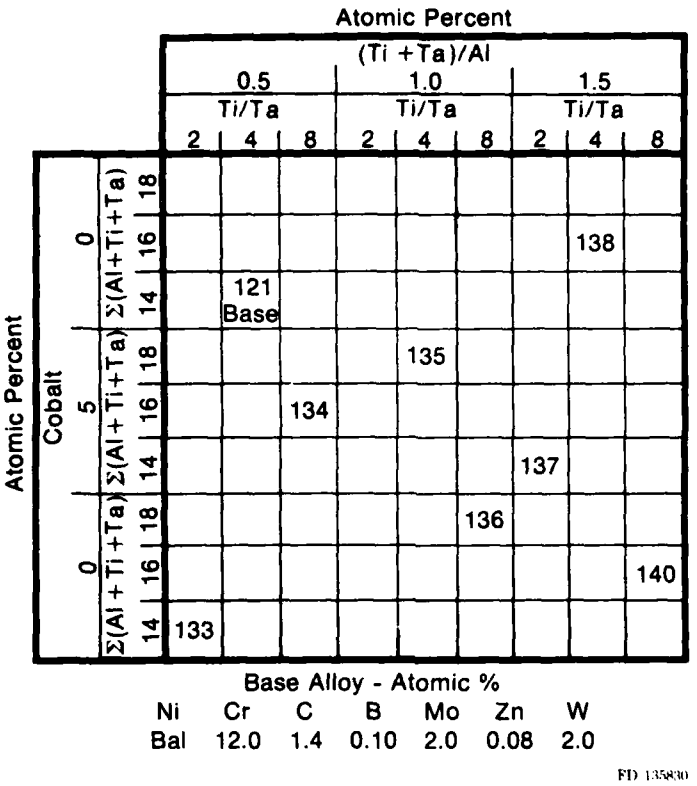

Figure 1. Analysis of γ′ in AF2-1DA Type Alloys

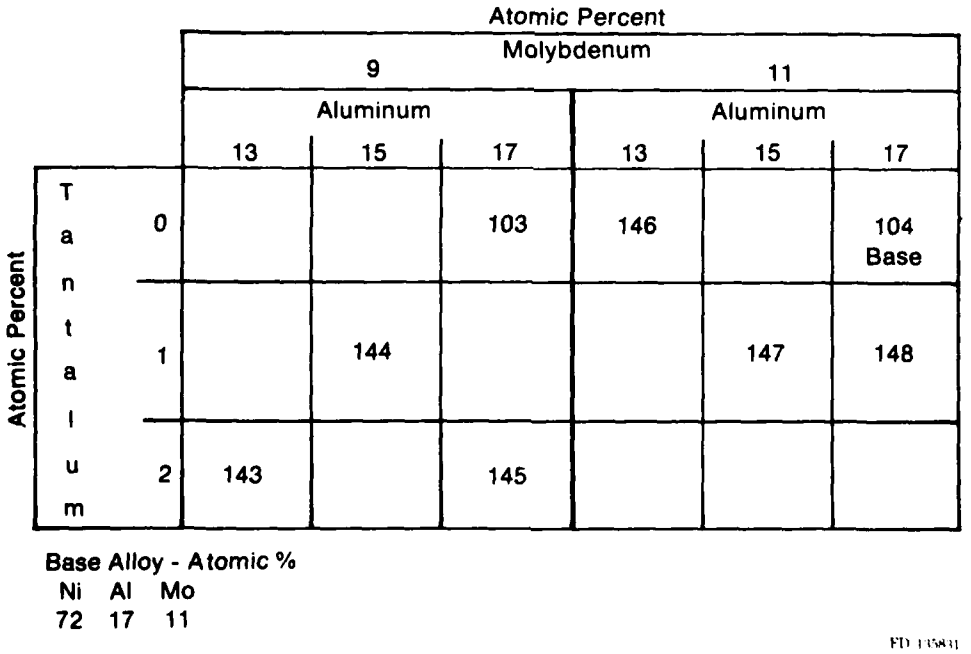

Figure 2. Analysis of Tantalum in Ni-Al-Mo Alloys

EXTRUSION

All of the previously noted alloys, with the exception of RSR 132 and 150, were extruded during this period for subsequent testing. Parameters for extrusions were selected with the intention of producing a fine grain, recrystallized product. Typically, reductions were high and process temperatures were about 0.8 to 0.9 of the secondary phase solvus.

We have standardized preparation of our materials for extrusion at this time and account for the following factors subsequent to producing the powder and prior to actual extrusion.

1. Transfer from the powder device to storage. We remove the powder material from the atomizing device under a slight positive pressure of He. The collection containers are unloaded in a He atmosphere chamber and the powders screened to separate all − 140 mesh (105 microns) from the coarser size fractions. The total oxygen plus moisture content in the chamber is typically 10 to 50 ppm. Once screened, the − 140 powders are loaded into glass containers, each fitted with a vacuum tight lid, and evacuated to somewhere probably on the order of 10 Torr. These containers are then stored. Each holds about 10 lb (4.5 kg). The lids can be checked visually to determine whether or not vacuum has been lost. If so, the material is removed from the current alloy study and marked for future possible use relative to effects of ambient exposure or subsequent material properties.

2. Transfer from storage to extrusion containers. When ready for use, the material is removed from its glass container in a helium atmosphere chamber and weighed into a stainless steel container which was designed to fit an outgassing device used for final evacuation. The steel container is filled to an amount which, by calculation, equals the total charge weight of the container to be used for extrusion. Both the transfer and extrusion container are sealed into the outgasser and operating parameters for degassing set at about 10^{-6} Torr and about 400°F (205°C). The material is transferred to the extrusion can at a rate of about 1 lb (0.45 Kg) per minute. Once the extrusion can is filled, the connecting tube from the can to the device is forge-sealed using a hydraulic press and an acetylene torch for heat.

The processing conditions and visual results of operation for the last 43 extrusions are listed in Table 2. All were extruded at AFML from a 3-in. liner. The majority processed with no difficulty. About 10% exhibited slight cracking, though not enough to prevent continued evaluation, and about 25% suffered major defects. The major defects were the result of either too severe working or melting at the extrusion temperature (as was the case for most of the Nb eutectics).

Other than as noted previously, the barstock was sound and showed no evidence of internal defects or particle boundary reaction. Typically, the stock was nearly complete or fully recrystallized, with grain sizes about ASTM 8 or finer. No spurious reactions were evident and particle bonding was complete in all cases. Oxygen and contaminant concentrations remained essentially the same as those reported in the previous report, i.e., O_2 less than 75 ppm, particle contaminant about 3 ppm, both satisfactory. Figure 3 shows examples of the as-extruded condition.

TABLE 2. EXTRUSION DATA

Alloy ID	Extrusion Temperature (°F)	(°C)	Reduction Ratio	Breakthrough Pressure (ksi)	(MPa)	Maximum Running Pressure (ksi)	(MPa)	Visual Appearance
95	2250	1232	43:1	151	1041	140	965	Good
96	2250	1232	43:1	154	1062	157	1083	Good
103	2300	1260	43:1	140	965	146	1006	Good
104	2300	1260	43:1	146	1006	151	1041	Good
104	2300	1260	43:1	140	965	138	952	Good
105	2300	1260	43:1	138	952	136	938	Good
108	2300	1260	43:1	151	1041	157	1083	Cracked
108	2250	1232	20:1	124	855	113	779	Good
108, 128	2250	1232	43:1	130	896	135	931	Cracked
109	2150	1177	43:1	162	1117	157	1083	Good
116	2300	1260	43:1	136	938	130	896	Good
120	2250	1232	43:1	154	1062	135	931	Slightly Cracked
128	2200	1204	43:1	146	1006	155	1089	Slightly Cracked
129	2250	1232	43:1	146	1006	135	931	Cracked
129	2200	1204	43:1	140	965	146	1006	Slightly Cracked
133	2250	1232	20:1	109	752	103	710	Good
133	2250	1232	43:1	130	896	135	931	Cracked
134	2250	1232	20:1	116	800	103	710	Good
134	2150	1177	43:1	165	1138	167	1151	Good
134	2250	1232	43:1	130	896	135	931	Cracked
135	2200	1204	20:1	124	855	119	821	Good
136	2250	1232	20:1	108	745	97	669	Good
137	2250	1232	20:1	124	855	105	724	Slightly Cracked
138	2200	1204	20:1	122	841	112	772	Slightly Cracked
140	2200	1204	20:1	135	931	108	745	Good
143	2300	1260	43:1	162	1117	163	1124	Good
143	2300	1260	43:1	140	965	140	965	Good
144	2300	1260	43:1	162	1117	167	1151	Good
144	2300	1260	43:1	149	1027	151	1041	Good
145	2300	1260	43:1	146	1006	135	931	Good
146	2250	1232	20:1	119	821	119	821	Good
146	2300	1260	43:1	132	910	105	724	Good
147	2300	1260	43:1	151	1041	151	1041	Good
147	2300	1260	43:1	134	924	124	855	Good
148	2300	1260	43:1	134	924	127	876	Good
149	2300	1260	43:1	140	965	138	952	Good
149	2360	1293	43:1	130	896	130	896	Cracked
151	2300	1260	43:1	135	931	135	931	Good
152	2300	1260	43:1	127	876	116	800	Melted
153	2250	1232	43:1	151	1041	162	1117	Melted
155	2300	1260	43:1	108	745	103	710	Melted
157	2300	1260	43:1	119	821	108	745	Melted
158	2300	1260	43:1	140	965	138	952	Good

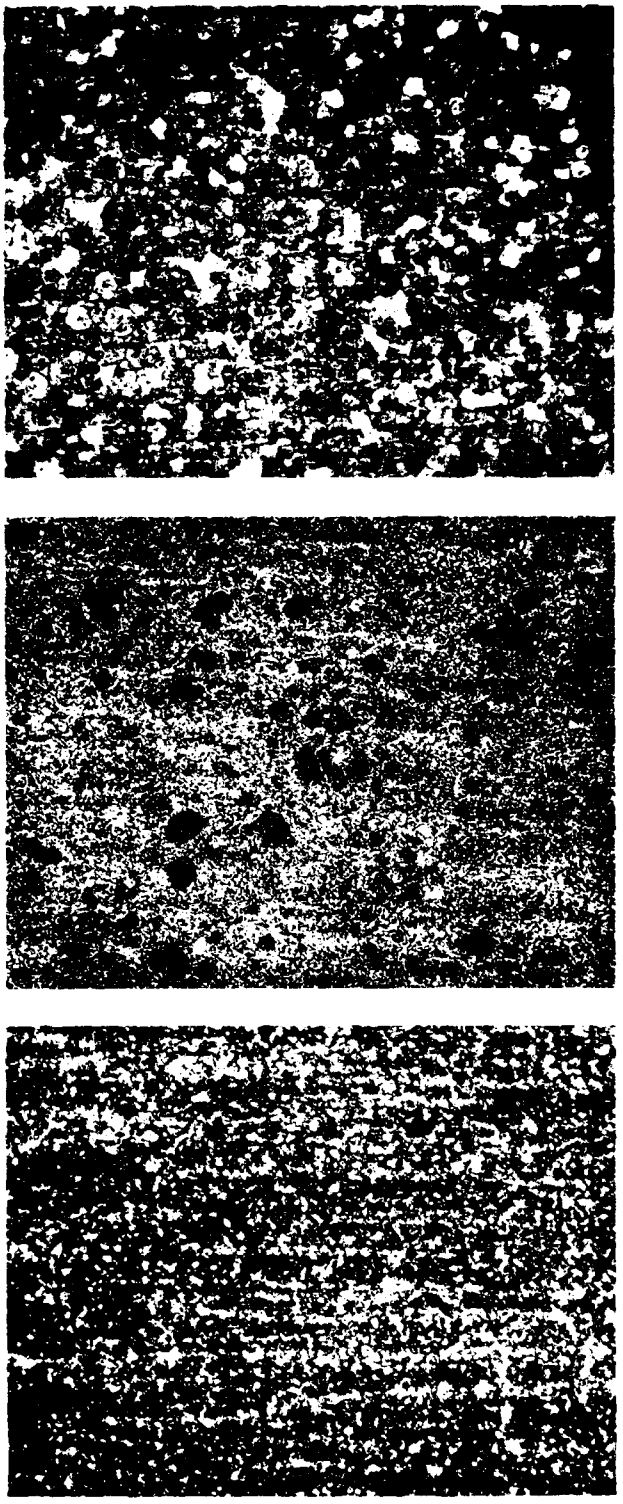

Figure 3. Experimental Superalloys as Extruded

ALIGNED GRAIN MICROSTRUCTURES

We are continuing to study abnormal grain growth with the experimental alloys in order to determine contributing factors from both composition and processing. A gradient furnace and two zone-annealing furnaces are being used for this purpose. The gradient furnace is capable of temperature gradients on the order of 100 to 150°F/in. (22 to 33 C/cm). The zone-annealing furnaces are set up to generate gradients anywhere from an order of magnitude smaller to an order of magnitude larger than the base furnace capability.

Table 3 summarizes the responses of the last 40 alloys to abnormal growth. As can be seen, 50% of the total group responded positively. The eutectic class did not respond at all, whereas highly effective responses were obtained for both category 3 and 4 compositions.

The extent of recrystallization resulting from the extrusion of the individual alloys was analyzed relative to the influence on subsequent abnormal growth. It was determined that, once nearly complete recrystallization was achieved, growth could commence. The lower bound observed to date is with alloy 123, which was about 85% recrystallized subsequent to extrusion, and which responded readily to abnormal growth. This factor of recrystallization obviously appears necessary but, at the same time, once it is satisfied, it does not appear to be the primary controlling mechanism.

The principle factor in achieving abnormal growth appears to us to be whether or not high-temperature dissolution of a secondary phase can be accomplished without incipient melting. For the 40 alloys listed in Table 3, the 20 which responded to abnormal growth all fell into this category. Of the 20 which did not, 14 of the compositions did not have a dissolving second phase.

Prior to dissolution, the second phase seems to act locally to pin the grain boundaries until such time as phase dissolution and thermal energy effects a release of grains to grow at the expense of smaller ones, with the driving force being reduction in grain boundary area.

The effect is shown in Figure 4. RSR 108 (MAR M200 composition) was used for the basic study. The sample which is depicted was being run under thermal gradient conditions conducive to abnormal growth and, halfway through the run, was quenched to suppress cool-down reactions. In the upper photo, which depicts essentially the as-extruded grain size, it is evident that the grain boundary volume includes a substantial concentration of secondary phase. In the lower photo, taken at the grain growth front, the second phase concentration is diminished from the boundary region and growth commences. Although no photographic evidence exists at this time, it is believed that similar conditions exist in the other categories of alloys.

The alignment of unusually large grains in alloys showing a propensity toward abnormal grain growth is accounted for by the thermal gradient existing at the growth front and the rate at which the gradient is moved. Our findings to date are limited in this respect but it seems likely that a criterion exists which places the product of thermal gradient and rate between some definable limits. These limits are not known presently but they do appear to be large enough that reasonable processing boundaries can be established. We plan to expand our effort in this area in order to better understand how control of growth and alignment can best be achieved.

Additional work with respect to grain alignment and orientation has also been carried out during the report period. In the previous report, we used X-ray diffraction procedures to identify the growth direction and reported it to be (110) for the conventional superalloy types. Since that time, further studies have been carried out which show that the (110) orientation is not a common feature for all alloys in the study. Figures 5 and 6 show the results obtained by Laue back reflection X-ray analysis for 7 different compositions, which represent not only the conventional superalloy compositions but also the Ni-Al-Mo series and the high γ alloys. Differences in preferred orientation are readily apparent.

TABLE 3. ALLOY RESPONSE TO ABNORMAL GRAIN GROWTH

Alloy	*Category**	*Response*
95	1	+
108	1	+
120	1	
121	1	+
122	1	+
124	1	+
129	1	
133	1	+
134	1	
135	1	
136	1	
137	1	
138	1	
140	1	
150	2	
152	2	
153	2	
155	2	
156	2	
157	2	
103	3	+
104	3	+
105	3	+
123	3	+
143	3	+
144	3	+
145	3	–
146	3	–
147	3	+
148	3	–
149	3	–
110	4	+
111	4	–
112	4	+
113	4	+
116	4	+
117	4	+
118	4	–
119	4	+
151	4	+

*Refer to Table 1

A. 0.5 mm From Growth Front

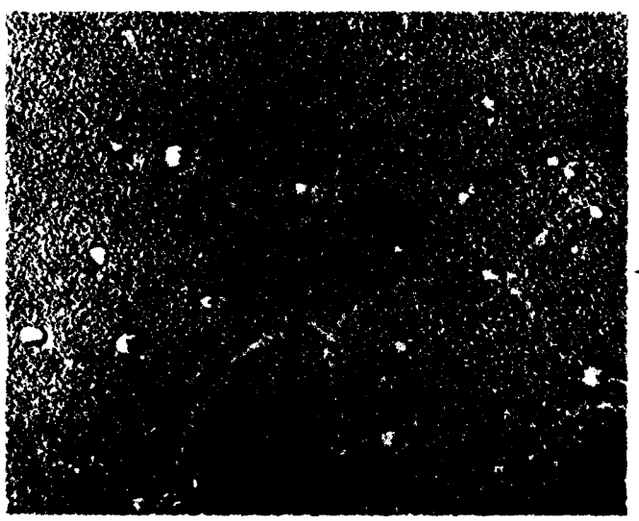

Mag: 3000X

B. At Growth Front
RSR 108

FD 135833

Figure 4. Effect of Grain Boundary Pinning on Abnormal Grain Growth

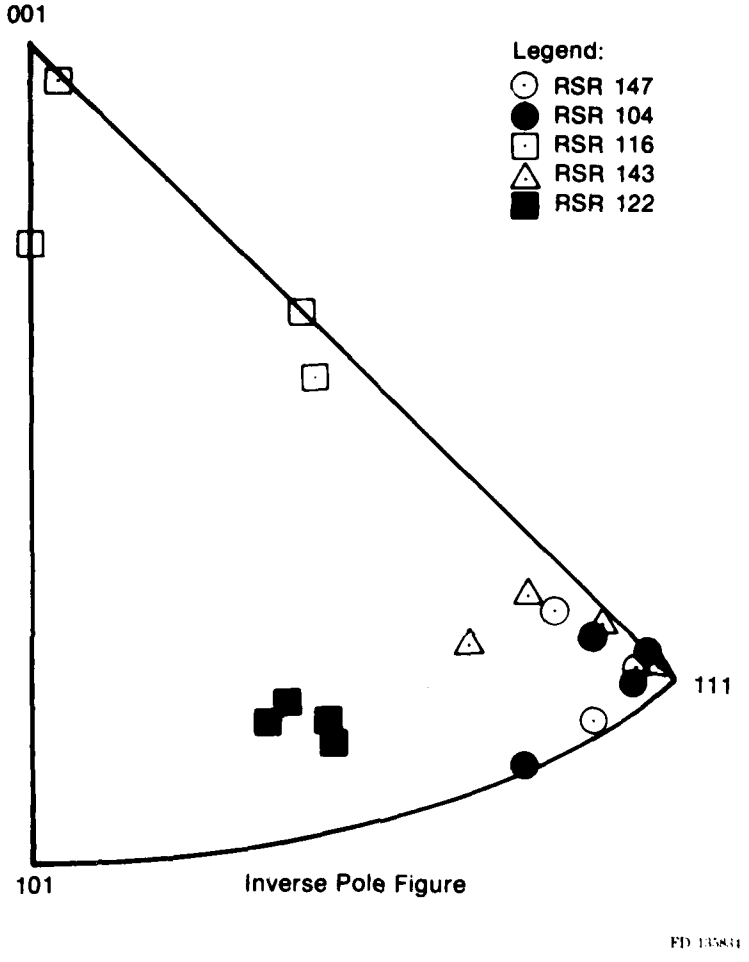

Figure 5. Orientation of Aligned Grain Structures in RSR 104, 116, 122, 143 and 147 Alloys

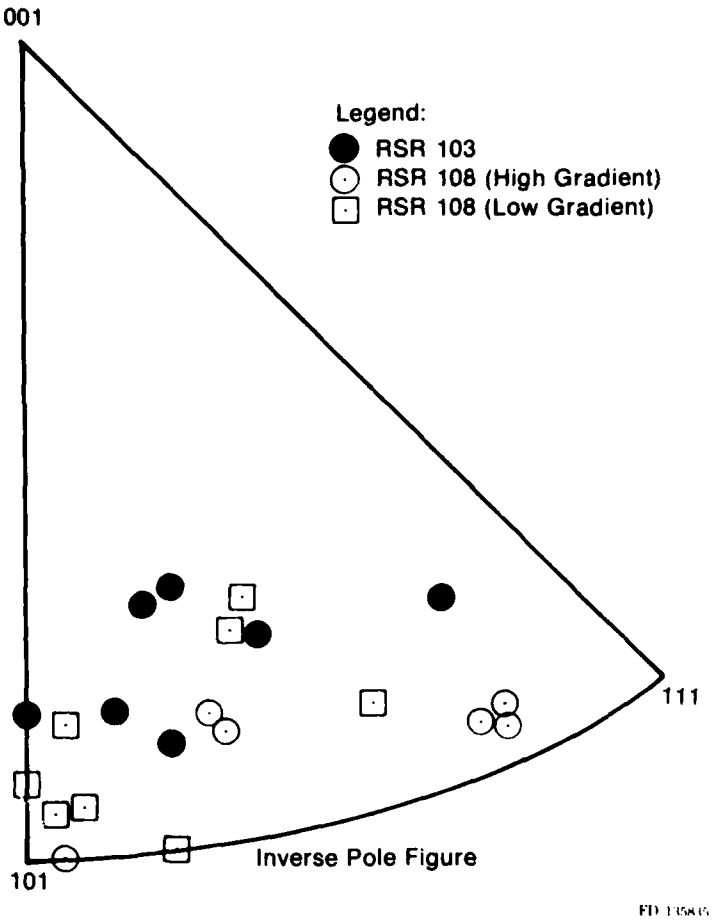

Figure 6. Orientation of Aligned Grain Structures in RSR 103 and 108 Alloys

The Ni-Al-Mo base alloys RSR 104, 143, and 147 have a strongly preferred (111) orientation, while RSR 103, an alloy of the same class, has a tendency toward (110). The high γ' alloy, RSR 116, has a tendency to (110). The conventional type alloys, RSR 122 and 108, tend toward (110), and, in the case of RSR 108 (the only case studied so far in this respect), it appears that that nature of thermal gradient can exert appreciable influence on overall alignment.

Several possibilities to account for these differences are being explored presently. RSR 103 has less Mo than the other 3 alloys in the series and it can be that the concentration difference alters the phases which subsequently control growth sufficiently to change the growth pattern. RSR 116 behaves in a manner similar to that reported for oxide dispersion-strengthened alloys. The presence of an insoluble carbide (based on 9.5 w/o W and 0.05 w/o C) could be acting in the same manner as the dispersed oxide. For the RSR 108 and 122 alloys, it can be speculated that the dissolution of γ' and the presence of a dispersed carbide combine to influence the final orientation.

Figures 7 and 8 add credibility to the contention of phase dissolution effects on growth. In Figure 7 is shown alloy 133, a conventional superalloy which contains both a dispersed carbide and a dissolving γ' phase.

In Figure 8 is shown alloy 143, a Ni-Al-Mo alloy modified with Ta which has a dissolving γ phase but no dispersed carbide. For the 133 alloy, grain growth appears almost as an explosive annihilation of fine grains by rapidly coarsening large grains. In the 143 alloy, growth almost seems to behave entirely differently and in a manner which simply suggests no impedance to reduction in grain boundary area. The presence (or absence) of phases is readily evident in the photos.

Texture in the as-extruded material was considered as a possible cause for the observed variations, however, in studies completed to date, we have not found indications of its existence. Figure 9 shows typical pinhole reflection patterns for 2 of the experimental alloys in the as-extruded form.

PHASE THERMAL STABILITY

Studies of phase thermal stability were continued during this period with the 3 classes of alloys exhibiting abnormal growth. We are using both isothermal and thermal gradients exposures from 1600°F (871°C) up to essentially T_m for this purpose, with times varying from 4 to 300 hours. Additionally, we are examining all creep-rupture test bars for indications of instability resulting from the combined factors of stress, temperature, and time.

In the conventional alloy series, both RSR 138 and 140 showed instability in the form of a massive reaction to η phase subsequent to exposures near 1600°F (871°C). The reaction is shown in Figure 10. The balance of alloys in the series showed no evidence of any deleterious reactions, for all conditions of exposure. The N_v calculations for 138 and 140 were 2.72 and 2.22, respectively, while N_v figures for the remaining alloys in the 130 to 140 series varied from 1.91 (RSR 133) to 2.76 (RSR 136). We were unable to produce an aligned grain structure in the highest N_v alloy and, therefore, have not conducted tests under stress with this composition. Whether or not an imposed stress would generate a similar reaction as observed with RSR 138 and 140 is conjecture. Suffice it to say that, in our application of N_v, no clear indication of stability was gained by its application.

In the high γ' series of alloys, no phase instability has been observed for any of the thermal and thermal-stress exposures and the work done in this period in this regard agrees with the results compiled in the previous report.

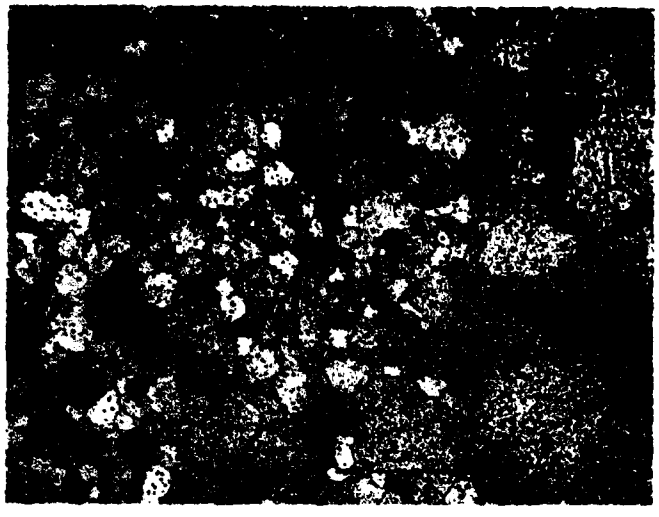

A. ~20°F (11°C) Below Coarsening Temperature

B. ~20°F (11°C) Above Coarsening Temperature

Mag: 400X
Kallings Reagent

FD 1688

Figure 7. Grain Growth in RSR 133

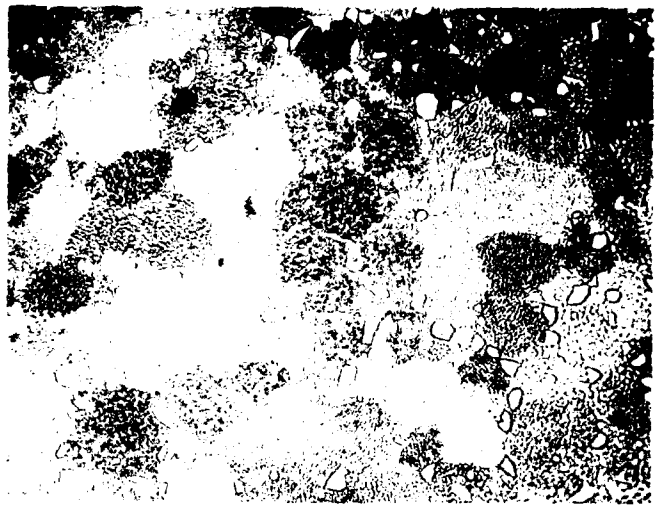

Mag: 400X

A. ~30°F (17°C) Below Grain Coarsening Temperature

Mag: 400X

B. ~30°F (17°C) Above Grain Coarsening Temperature

Figure 8. Grain Growth in RSR 143

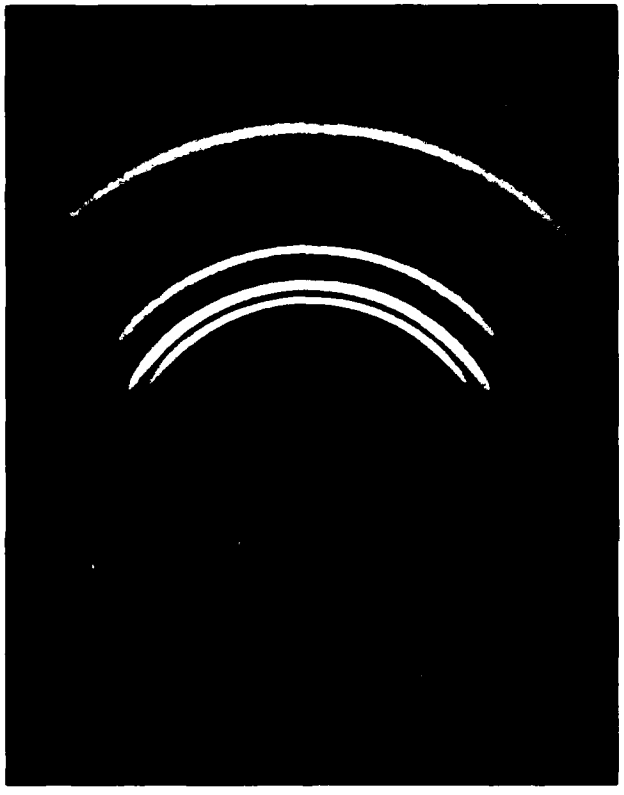

RSR 101

RSR 103

Pinhole Reflection Patterns
As - Extruded Condition

Figure 9. Absence of Texture in Extruded Starting Stock

Mag: 400X
Kallings Reagent
Subsequent to Annealing and 50-hr Exposure at ~1600°F (871°C)
FD 135841

Figure 10. Low Temperature Instability in RSR 138

Grain boundary phase instability was noted in creep-rupture specimens of RSR 104 alloy, as shown in Figure 11, and is a condition which we believe was a part of the failure mechanism. The reaction was a localized and accelerated coarsening of the same phases which are present in the alloy matrix. The coarsening tendency was most evident in the higher Mo alloys of the 103 to 123 group and the purpose of the previously mentioned Ta modifications to this series was, in part, to negate this reaction by elemental substitution of Ta, either at the expense of Mo or by improving the basic stability of the γ' phase.

The results of the Ta addition relative to grain boundary stability are shown in Figure 12. The samples depicted were annealed near 2400°F (1315°C) and were subsequently exposed for 50 hours at 2000°F (1093°C). Also, the samples used were equiaxed bars cut from as-extruded stock, with relatively high-energy grain boundaries compared to the tilt boundaries in the aligned grain structures. It is evident from the photos that additions of Ta, with concurrent reductions of Al and Mo (but not at the expense of total γ' concentration), reverse the unstable nature of the grain boundaries to a condition of stability well within the bounds of engineering usefulness. Applied stress might be a contributing factor to the overall stability of grain boundaries in this entire class of alloys and we are currently running tests to ascertain its influence.

The stable characteristic of the RSR 143 alloy over the RSR 104-type compositions is accompanied by significant differences in phases and phase morphology, which could be the principle factors for eliminating the rapid grain boundary phase coarsening. This is illustrated by the 4 transmission electron micrographs shown in Figure 13. RSR 104, after undergoing abnormal growth and air-cooling from the growth temperatures, is shown in dark field in Figure 13A. This structure is analogous to the RSR 143 structure shown in Figure 13B. The RSR 104 structure consists of γ' cells surrounded by a complex cell wall structure. The cell walls contain long Mo precipitates in a $\gamma - \gamma'$ matrix. This matrix also contains a very fine precipitate which has been identified as domains of metastable Ni_2Mo. The analogous RSR 143 structure consists of a fine array of faults in a γ' matrix. Microbeam X-ray analysis shows Ta to be segregated preferentially to the γ' and Mo to the faults. The dark field shows a fine precipitate associated with these faults, and is probably an ordering structure such as that in RSR 104. Note that no cell wall structure or Mo precipitate is present.

Mag: 100X

Failed After 172 hr at 1800°F (982°C) and 30 ksi (206.8 MPa)

FD 135840

Figure 11. Grain Boundary Contribution to Creep-Rupture Failure in RSR 104

When the structure of Figure 13A is exposed at a lower temperature, the structure shown in Figure 13C results. This sample is an RSR 103 alloy but is qualitatively the same as RSR 104. The structure consists of a continuous γ' matrix, which contains Mo precipitates and some isolated regions of a fine mixture of γ and γ'. This is in strong contrast with the structure of RSR 143, shown in Figure 13D and obtained after an equivalent heat treatment. This structure exhibits the $\gamma - \gamma'$ cell-type morphology, the cells being γ' and the walls a complex $\gamma - \gamma'$ precipitate structure. The γ' cells are not continuous as is evident in the 103 alloy and there is no Mo precipitate present in the cell walls. The precipitate in the cell walls is a fine, ~100A scale, domain structure which is probably a Ni-Mo-ordered compound. The cell walls also contain a considerable amount of γ'.

An important aspect of the RSR 143 structural evolution with respect to high-temperature behavior is that the extremely fine scale precipitate apparently has been stabilized to the extent that it should be an important factor, not only to bulk alloy stability, but also to creep resistance of the material. Another significant feature between the 2 alloys is that the RSR 104 types form a continuous γ' matrix while RSR 143 does not. Thus, it can be expected that the 143 alloy would behave in a manner more akin to conventional superalloys than would 103 or 104, which have the continuous γ' intermetallic matrix.

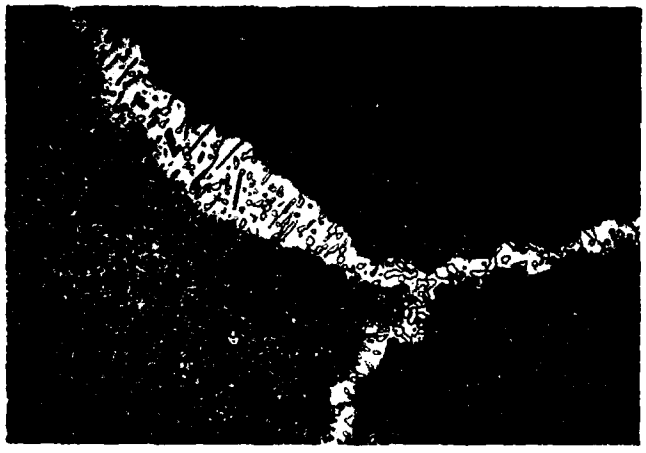

RSR 104 -
8Al-18Mo-OTa

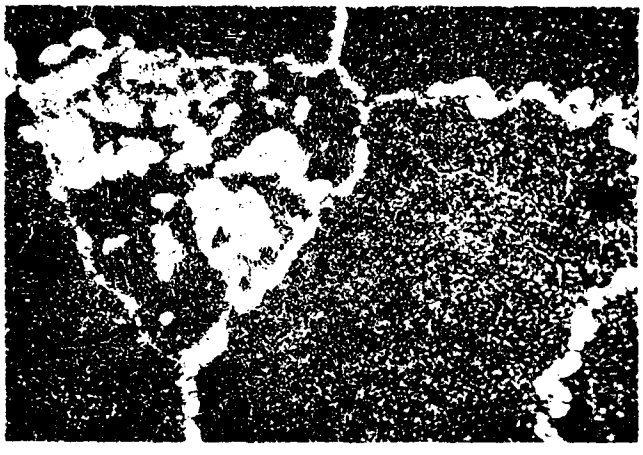

RSR 144 -
7Al-15Mo-3Ta

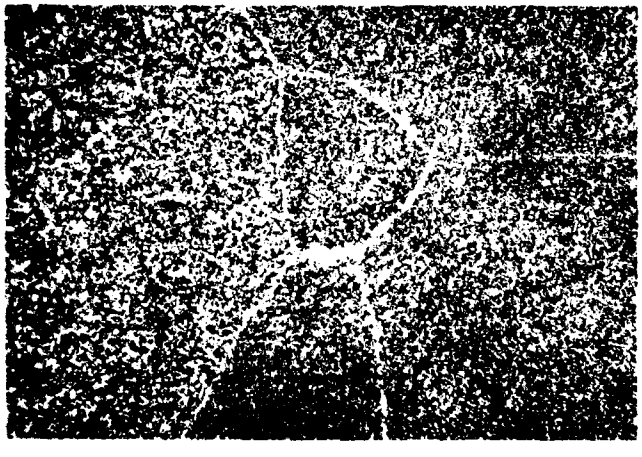

RSR 143 -
6Al-14Mo-6Ta

Mag: 400X
Kallings Reagent

Note: Subsequent to Annealing and 50-hr Exposure at 2000°F (1093°C)

FD 135842

Figure 12. Grain Boundary Stability Characteristics in the RSR 104 and RSR 143 Type Alloys

Mag: 50,000X
RSR 104 2400°F (1315°C) Anneal

Mag: 29,000X
RSR 143 2400°F (1315°C) Anneal

Mag: 50,000X
RSR 103 2400°F (1315°C) Anneal + 1900°F (1038°C)/44-hr

Mag: 29,000X
RSR 143 2400°F (1315°C) Anneal +2000°F (1093°C)/50-hr

FD 135843

Figure 13. Microstructure of RSR 104 and 143 Type Alloys

TEST RESULTS WITH ALIGNED GRAIN STRUCTURES

Seven alloys which responded effectively to zone annealing were tested during this period. The heat treatments, depending on the class of material, were the same as reported in the previous report. Test conditions were selected in order to complement and add to the data already reported. The results are listed in Table 4.

TABLE 4. CREEP-RUPTURE RESULTS OF RSR ALLOYS HAVING ALIGNED GRAIN STRUCTURES

ID	Temperature °F	°C	Stress (ksi)	MPa	1% (hr)	Life (hr)	El %	Minimum Creep Rate (hr^{-1} × 10^{-5})
108	1400	760	100	689	2.7	19.7	8.1	18
108	1800	982	30	207	67.4	86.7	7.1	6
108	2000	1093	15	103	11.6	14.2	8.3	52
103	1800	982	30	207	12.0	44.7	14.8	77
104	1400	760	90	621	205.4	464.3	7.0	3
104	1800	982	30	207	71.2	172.4	9.7	7
105	1400	760	90	621	101.0	129.7	3.9	6
105	1800	982	30	207	92.4	110.6	1.7	6
143	1800	982	30	207	On Test			0.2
143	1900	1038	30	207	On Test			3
144	1800	982	30	207	156	161.4	1.9	4
144	1900	1038	30	207	-	12.1	5.1	-
147	1800	982	30	207	~450	526.9	N/R	1

The 103 to 147 series continue to look attractive relative to program goals. Probably of most interest is the creep rate associated with the high-temperature testing of RSR 143. The tests are still in progress but, after confirming that the samples were in 2nd-stage creep, it is evident that the structure of the material as described previously has imparted creep resistance which is substantially better than one would anticipate.

We are examining the failed specimens in order to determine the individual roles of grains, grain alignment variations, and grain boundaries in the failure process. To date, we have not separated the three in a manner so precise as to permit quantified contributions. We do feel, however, that our analyses are sufficiently complete that it can be stated that the alignment matches and grain boundary involvement (phase stable) are satisfactory for the intended purposes of application.

Other than the heat-treatment parameters needed to achieve aligned grain structures and desired phase solutioning, thermal processing to obtain the best combination of strength and ductility has been held in abeyance. We have started major activities in this area and plan to include total heat treat response in future analyses of overall alloy utility.

FORGEABILITY

Since the start of the program, most of the alloys have been subjected to deformation under parameters implied by the GATORIZING® forge process. All indications suggest that no difficulty will be encountered in deforming any of the materials to net shape forms.

Because of a presently high interest in the RSR 104-type alloy, we expounded upon the deformation features of this alloy through comprehensive flow stress and deformation measurements. For this purpose, we used alloy stock which was extruded 43/1 at 2200°F (1204°C) and which, subsequently, had a fully recrystallized structure with an average grain size of ASTM 14 Standard tensile samples were used in this study and results of testing are shown in Figure 14.

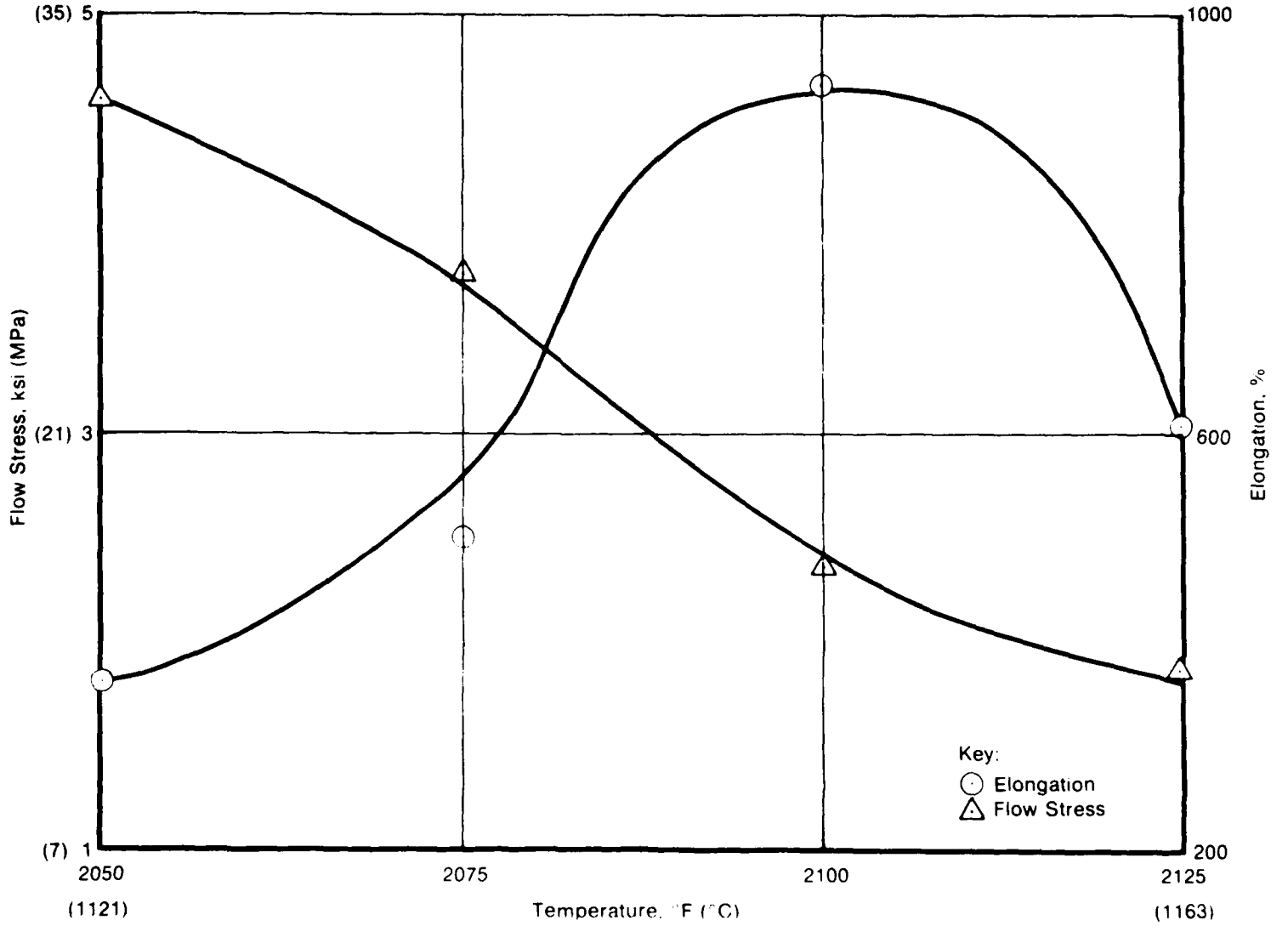

Figure 14. Superplastic Behavior of Extruded RSR 104

Maximum elongation was achieved at 2100°F (1149°C) while flow stress continued to drop off to under 2 ksi (14 MPa) at 2125°F (1163°C). No grain growth occurred during testing and tests in inert atmosphere showed that the ambient environment used for the testing reported in the figure did not interfere with the final results. These results indicate to us that, even though we are studying alloys of very high incipient melt and secondary phase dissolution temperatures, we are not imposing a constraint to existing processing methods which would negate otherwise satisfactory achievement.

SECTION III

ON-GOING STUDY

On the basis of test and microstructural data obtained during this and the previous report periods, we are expanding our alloy development activities into 2 principal categories: (1) alloys based on Ni-Al-Mo and, (2) alloys of high γ' concentration. Work with the classical eutectic compositions is being discontinued. Work with the conventional alloys will be confined primarily to study of heat treat responses. Additionally, during this forthcoming period, we plan to pursue identification of alloy features which promote stability and how heat treat can alter observed test properties. Finally, we plan to initiate studies related to actual fabrication of turbine airfoils, with particular interest in the interrelationship of various processing steps to final part quality and alloy integrity.


DATE:
TIME